

JHU-TIPAC-96022

MADPH-97-994

hep-ph/9707365

## Leptoproduction of $J/\psi$

Sean Fleming \*

*Department of Physics, University of Wisconsin, Madison**Madison, Wisconsin 53706 U.S.A.*

fleming@pheno.physics.wisc.edu

Thomas Mehen †

*Department of Physics and Astronomy, The Johns Hopkins University**3400 North Charles Street, Baltimore, Maryland 21218 U.S.A.*

mehen@dirac.pha.jhu.edu

(July 1997)

### Abstract

We study leptoproduction of  $J/\psi$  at large  $Q^2$  within the nonrelativistic QCD (NRQCD) factorization formalism. The cross section is dominated by color-octet terms that are of order  $\alpha_s$ . The color-singlet term, which is of order  $\alpha_s^2$ , is shown to be a small contribution to the total cross section. We also calculate the tree diagrams for color-octet production at order  $\alpha_s^2$  in a region

---

\*address after Sept. 1 1997: University of Toronto, 60 St. George St., Toronto, Ontario CA, M5S1A7

†address after Sept. 1 1997: California Institute of Technology, Pasadena, CA 91125

of phase space where there is no leading color-octet contribution. We find that in this regime the color-singlet contribution dominates. We argue that non-perturbative corrections arising from diffractive leptonproduction, higher twist effects, and higher order terms in the NRQCD velocity expansion should be suppressed as  $Q^2$  is increased. Therefore, the color-octet matrix elements  $\langle \mathcal{O}_8^\psi(^1S_0) \rangle$  and  $\langle \mathcal{O}_8^\psi(^3P_0) \rangle$  can be reliably extracted from this process. Finally, we point out that an experimental measurement of the polarization of leptonproduced  $J/\psi$  will provide an excellent test of the NRQCD factorization formalism.

## I. INTRODUCTION

Quarkonium production has been the focus of much experimental and theoretical attention in recent years. This surge in interest is largely due to the observation of gross discrepancies between experimental measurements of  $J/\psi$  and  $\psi'$  production at the Collider Detector Facility (CDF) at the Fermilab Tevatron [1] and calculations based on the Color-Singlet Model [2]. The dramatic failure of the traditional technique for calculating quarkonia production and decay rates has led to a new paradigm for understanding quarkonia: the nonrelativistic QCD (NRQCD) factorization formalism of Bodwin, Braaten, and Lepage [3].

A central result of the NRQCD factorization formalism is that inclusive quarkonium production cross sections have the form of a sum of products of short-distance coefficients and NRQCD matrix elements. The short-distance coefficients are associated with the production of a heavy quark-antiquark pair in specific color and angular-momentum states. They can be calculated using ordinary perturbative techniques. The NRQCD matrix elements parameterize the effect of long-distance physics such as the hadronization of the quark-antiquark pair. These can be determined phenomenologically.

The power of the NRQCD formalism stems from the fact that factorization formulas for observables are expansions in the small parameter  $v$ , where  $v$  is the average relative velocity of the heavy quark and anti-quark in the quarkonium bound state. For charmonium  $v^2 \sim 0.3$ , and for bottomonium  $v^2 \sim 0.1$ . NRQCD  $v$ -scaling rules [4] allow us to estimate the relative sizes of various NRQCD matrix elements. This information, along with the dependence of the short-distance coefficients on  $\alpha_s$  and  $\alpha$ , permits us to decide which terms must be retained in expressions for observables to reach a given level of accuracy. At low orders, factorization formulas involve only a few matrix elements, so several observables can be related by a small number of parameters.

Prior to the innovations presented in Ref. [3], most  $J/\psi$  production calculations took into account only the hadronization of  $c\bar{c}$  pairs initially produced in a color-singlet  $^3S_1$  state, as parameterized by the NRQCD matrix element  $\langle \mathcal{O}_1^\psi(^3S_1) \rangle$ . An important aspect of the

NRQCD formalism is that, in addition to the color-singlet contribution, it allows for the possibility that a  $c\bar{c}$  pair produced in a color-octet state can evolve nonperturbatively into a  $J/\psi$  or  $\psi'$ . This color-octet mechanism is central to the current theoretical understanding of charmonium production at the Tevatron.

For a majority of phenomenological applications of the NRQCD factorization formalism, the most important color-octet matrix elements are  $\langle\mathcal{O}_8^\psi(^3S_1)\rangle$ ,  $\langle\mathcal{O}_8^\psi(^1S_0)\rangle$ , and  $\langle\mathcal{O}_8^\psi(^3P_J)\rangle$ . They describe the non-perturbative evolution of a color-octet  $c\bar{c}$  pair in either a  $^3S_1$ ,  $^1S_0$ , or  $^3P_J$  angular momentum state into a  $J/\psi$ . Using heavy quark spin symmetry relations [3], it is possible to express all three P-wave matrix elements in terms of one:  $\langle\mathcal{O}_8^\psi(^3P_J)\rangle = (2J+1)\langle\mathcal{O}_8^\psi(^3P_0)\rangle + O(v^2)$ . Thus, at leading order in  $v$ , there are three color-octet matrix elements. At this time they cannot be computed from first principles, and must therefore be extracted from experimental data.

The most precise determination of the color-octet matrix element  $\langle\mathcal{O}_8^\psi(^3S_1)\rangle$  comes from a fit of a leading order theoretical calculation [5,6] to CDF data on  $J/\psi$  production at high transverse momentum ( $P_\perp$ ). A linear combination of the remaining two color-octet matrix elements  $\langle\mathcal{O}_8^\psi(^1S_0)\rangle$  and  $\langle\mathcal{O}_8^\psi(^3P_0)\rangle$  can also be determined by fitting the leading order calculation to CDF data on  $J/\psi$  produced at low to moderate  $P_\perp$ . The fit is extremely sensitive to theoretical uncertainties, so that the value determined for the linear combination of  $\langle\mathcal{O}_8^\psi(^1S_0)\rangle$  and  $\langle\mathcal{O}_8^\psi(^3P_0)\rangle$  can only be regarded as an order of magnitude estimate. There are other  $J/\psi$  production processes, such as those measured at fixed target experiments in photonic [7], and hadronic [8] collisions, that could, in principle, provide a means to determine  $\langle\mathcal{O}_8^\psi(^1S_0)\rangle$  and  $\langle\mathcal{O}_8^\psi(^3P_0)\rangle$ . However, in each case there are large theoretical uncertainties that only allow for an order of magnitude estimate of these color-octet matrix elements.

It is clear that testing the NRQCD factorization formalism requires a precise determination of each of the leading matrix elements. Specifically, the challenge lies in an accurate measurement of  $\langle\mathcal{O}_8^\psi(^1S_0)\rangle$  and  $\langle\mathcal{O}_8^\psi(^3P_0)\rangle$ . In this paper we study leptonproduction of  $J/\psi$ , and show that it is possible to determine these matrix elements from a measurement of the

unpolarized  $J/\psi$  production cross section. We also show that once these matrix elements are extracted, the polarization of the  $J/\psi$  can be predicted without introducing any new parameters. Thus, a measurement of the polarization of lepton-produced  $J/\psi$  will provide an excellent test of the NRQCD factorization formalism.

An explicit calculation need not be carried out to understand why it should be possible to determine  $\langle \mathcal{O}_8^\psi(^1S_0) \rangle$  and  $\langle \mathcal{O}_8^\psi(^3P_0) \rangle$  from a measurement of the  $J/\psi$  lepton-production cross section. The  $O(\alpha_s)$  contribution to  $J/\psi$  production comes from processes in which the  $c\bar{c}$  pair is produced at short-distances in either a color-octet  $^1S_0$  or  $^3P_J$  configuration. It is not until one includes the  $O(\alpha_s^2)$  contributions that it is possible for  $J/\psi$  to be produced through the production at short distances of a  $c\bar{c}$  pair in a color-singlet  $^3S_1$  state. The color-octet matrix elements  $\langle \mathcal{O}_8^\psi(^1S_0) \rangle$  and  $\langle \mathcal{O}_8^\psi(^3P_0) \rangle$  are suppressed by  $v^3$  and  $v^4$ , respectively, relative to the color-singlet matrix element. Since the perturbative coefficient for color-octet production is enhanced relative to the perturbative coefficient for color-singlet production by a factor of  $\sim \pi/\alpha_s$ , we expect the color-octet contribution to be roughly  $v^3\pi/\alpha_s \approx 2$  times the color-singlet contribution. In fact, upon completing the calculation, we find that color-octet contribution is about 4 times the size of the leading order color-singlet contribution.

Note that since  $Q^2$  can be large, lepton-production is a better process from which to extract  $\langle \mathcal{O}_8^\psi(^1S_0) \rangle$  and  $\langle \mathcal{O}_8^\psi(^3P_0) \rangle$  than photoproduction and low-energy hadroproduction. The latter two processes lack any large scale other than the charm quark mass, and consequently, perturbative corrections to leading order calculations are larger. In addition nonperturbative effects, such as higher twist corrections to the parton model and diffractive  $J/\psi$  production, are less effectively suppressed in photoproduction and low-energy hadroproduction than in lepton-production at large  $Q^2$ .

Finally, we point out that there are  $J/\psi$  lepton-production final states which can only be described by  $O(\alpha_s^2)$  tree-level contributions (*i.e.* there is no  $O(\alpha_s)$  color-octet contribution). The final states are those in which a gluon jet is well separated from the  $J/\psi$ . Though the dominant contribution to these final states comes from the  $O(\alpha_s^2)$  color-singlet term, there are also  $O(\alpha_s^2)$  color-octet contributions. We calculate these color-octet terms to determine

if there is any region of phase space where they are enhanced relative to the color-singlet term. We find that in the regime where the calculation is valid the color-singlet term always dominates.

This paper is organized in such a way as to separate theory from phenomenology. Readers who are only interested in the phenomenological implications of this work can skip the theoretical discussion without loss of coherence.

We discuss theoretical issues in sections II–IV. First, we briefly review the NRQCD factorization formalism. Then we present the  $O(\alpha_s)$  and  $O(\alpha_s^2)$  tree level calculations of  $J/\psi$  leptonproduction. At  $O(\alpha_s)$ , we calculate both the polarized and unpolarized  $J/\psi$  production cross sections. Finally, we discuss possible corrections to our calculations from diffractive production and higher twist corrections to the parton model. We also address the possibility of a breakdown of the NRQCD velocity expansion near the boundaries of phase space. For the distributions computed in this paper, we argue that these errors are systematically reduced as  $Q^2$  is made large.

The phenomenology of  $J/\psi$  leptonproduction is presented in sections V and VI. First, we discuss the present status of the determination of the leading order NRQCD matrix elements. Then we present our predictions, and discuss the theoretical limitations on the accuracy to which  $\langle \mathcal{O}_8^\psi(^1S_0) \rangle$  and  $\langle \mathcal{O}_8^\psi(^3P_0) \rangle$  can be measured in leptonproduction. We conclude that leptonproduction of unpolarized  $J/\psi$  is an excellent way to measure  $\langle \mathcal{O}_8^\psi(^1S_0) \rangle$  and  $\langle \mathcal{O}_8^\psi(^3P_0) \rangle$ , and that leptonproduction of polarized  $J/\psi$  provides a powerful test of the NRQCD factorization formalism.

## II. THE NRQCD FACTORIZATION FORMALISM

The NRQCD factorization formalism of Bodwin, Braaten, and Lepage [3] has emerged as a new paradigm for computing the production and decay rates of heavy quarkonia. This formalism provides a rigorous theoretical framework which systematically incorporates relativistic corrections and ensures the infrared safety of perturbative calculations [9]. In the

NRQCD factorization formalism, cross sections for the production of a quarkonium state  $H$  are written as

$$\sigma(H) = \sum_n \frac{F_n}{m_Q^{d_n-4}} \langle 0 | \mathcal{O}_n^H | 0 \rangle, \quad (1)$$

where  $m_Q$  is the mass of the heavy quark  $Q$ . The short-distance coefficients,  $F_n$ , are associated with the production, at distances of order  $1/m_Q$  or less, of a  $Q\bar{Q}$  pair with quantum numbers indexed by  $n$  (angular momentum  $^{2S+1}L_J$  and color 1 or 8). They are computable in perturbation theory. In Eq. (1),  $\langle 0 | \mathcal{O}_n^H | 0 \rangle$  are vacuum matrix elements of NRQCD operators:

$$\langle 0 | \mathcal{O}_n^H | 0 \rangle \equiv \sum_X \sum_\lambda \langle 0 | \mathcal{K}_n^\dagger | H(\lambda) + X \rangle \langle H(\lambda) + X | \mathcal{K}_n | 0 \rangle, \quad (2)$$

where  $\mathcal{K}_n$  is a bilinear in heavy quark fields which creates a  $Q\bar{Q}$  pair in an angular-momentum and color configuration indexed by  $n$ . The bilinear combination  $\mathcal{K}_n^\dagger \mathcal{K}_n$  has energy dimension  $d_n$ . The production matrix elements describe the evolution of the  $Q\bar{Q}$  pair into a final state containing the quarkonium  $H$  plus additional hadrons ( $X$ ) which are soft in the quarkonium rest frame.

Throughout the remainder of the paper, we use a shorthand notation in which the vacuum matrix elements are written as  $\langle \mathcal{O}_{(1,8)}^H(^{2S+1}L_J) \rangle$ .

The NRQCD matrix elements obey simple scaling laws [4] with respect to  $v$ , the relative velocity of the  $Q$  and  $\bar{Q}$ . Therefore, Eq. (1) is a double expansion in  $v$  and  $\alpha_s$ . Since the NRQCD matrix elements are sensitive only to large distance scales they are independent of the short-distance process in which the  $Q$  and  $\bar{Q}$  are produced. Thus, it is possible to extract numerical values for the NRQCD matrix elements in one experiment and use them to predict production cross sections in other processes.

### III. LEPTOPRODUCTION CALCULATION

At leading order in  $\alpha_s$ ,  $J/\psi$  are produced through the hadronization of a  $c\bar{c}$  pair in either a  $^1S_0$ , or  $^3P_J$  configuration. The Feynman diagrams are shown in Fig. 1.

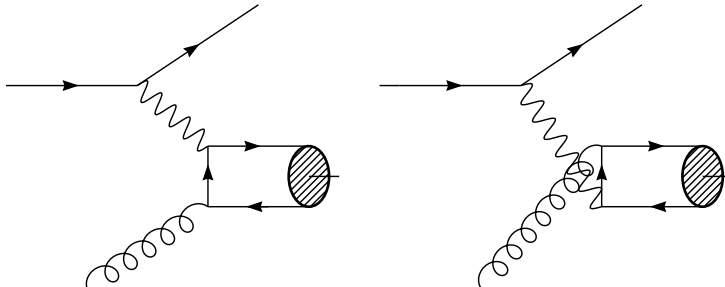


FIG. 1. Leading order diagrams for color-octet leptoproduction of  $J/\psi$

Theoretical predictions for the  $J/\psi$  leptoproduction cross section can be computed using the techniques of Ref. [10]. The short-distance coefficients appearing in Eq. (1) can be computed by matching a perturbative calculation in full QCD with a corresponding perturbative calculation in NRQCD. The production cross section of a  $c\bar{c}$  pair with relative three-momentum  $\mathbf{q}$  is computed in full QCD, and Taylor expanded in powers of  $\mathbf{q}$ . In this Taylor expansion, the four-component Dirac spinors are expressed in terms of nonrelativistic two-component heavy quark spinors. The NRQCD matrix elements on the right-hand side of Eq. (1) are easily expressed in terms of the two-component heavy quark spinors and powers of  $\mathbf{q}$ . The  $F_n$  appearing in Eq. (1) are then chosen so that the full QCD calculations and NRQCD calculations agree. Detailed examples of the calculational technique can be found in Ref. [10]; here we will merely quote our result for the differential cross section.

The expression for the cross section determined from the diagrams in Fig. 1 is

$$\begin{aligned} \sigma(e + p \rightarrow e + \psi + X) &= \int \frac{dQ^2}{Q^2} \int dy \int dx f_{g/p}(x) \delta(xys - (2m_c)^2 - Q^2) \\ &\times \frac{2\alpha_s(\mu^2)\alpha^2 e_c^2 \pi^2}{m_c(Q^2 + (2m_c)^2)} \left\{ \frac{1 + (1 - y)^2}{y} \left[ \langle \mathcal{O}_8^\psi(^1S_0) \rangle + \frac{3Q^2 + 7(2m_c)^2}{Q^2 + (2m_c)^2} \frac{\langle \mathcal{O}_8^\psi(^3P_0) \rangle}{m_c^2} \right] \right. \\ &\quad \left. - y \frac{8(2m_c)^2 Q^2}{(Q^2 + (2m_c)^2)^2} \frac{\langle \mathcal{O}_8^\psi(^3P_0) \rangle}{m_c^2} \right\}, \end{aligned} \quad (3)$$

where  $s$  is the electron-proton center-of-mass energy squared,  $\mu^2 = Q^2 + (2m_c)^2$  is both the factorization and renormalization scale, and  $f_{g/p}(x)$  is the gluon distribution function of the proton. The momentum fraction of the virtual photon relative to the incoming lepton is  $y \equiv P_p \cdot q / P_p \cdot k$ , where  $P_p$  is the proton four-momentum,  $q$  is the photon four-momentum, and



$k$  is the incoming lepton four-momentum, and  $Q^2 \equiv -q^2$ . Note that the relative importance of  $\langle \mathcal{O}_8^\psi(^1S_0) \rangle$  and  $\langle \mathcal{O}_8^\psi(^3P_0) \rangle$  changes as a function of  $Q^2$ . Thus it is possible to fit the differential cross section as a function of  $Q^2$  and extract both of these matrix elements.

The result presented in Eq. (3) holds for all values of  $Q^2$ . Taking the limit  $Q^2 \rightarrow 0$  one recovers the photoproduction cross section [7] convoluted with the electron splitting function:

$$\lim_{Q^2 \rightarrow 0} \sigma(e + P \rightarrow e + \psi + X) \rightarrow \frac{\alpha}{2\pi} \int \frac{dQ^2}{Q^2} \int_0^1 dy \frac{1 + (1-y)^2}{y} \hat{\sigma}(\gamma + P \rightarrow \psi + X). \quad (4)$$

As mentioned in the introduction, corrections to the photoproduction cross section from higher order perturbative QCD corrections terms, from diffractive photoproduction, and from higher twist effects, may all be large. However, in the high-energy limit  $Q^2, s \gg (2m_c)^2$  we expect corrections to be negligible. Letting  $Q^2, s \gg (2m_c)^2$  in Eq. (3) we obtain

$$\begin{aligned} \lim_{m_c^2/Q^2, m_c^2/s \rightarrow 0} \sigma(e + P \rightarrow e + \psi + X) &\rightarrow \int \frac{dQ^2}{Q^2} \int dy \int dx f_{g/N}(x) \delta(xys - Q^2) \\ &\times \frac{2\alpha_s(Q^2)\alpha^2 e_c^2 \pi^2}{m_c Q^2} \frac{1 + (1-y)^2}{y} \left( \langle \mathcal{O}_8^\psi(^1S_0) \rangle + 3 \frac{\langle \mathcal{O}_8^\psi(^3P_0) \rangle}{m_c^2} \right). \end{aligned} \quad (5)$$

Once the color-octet matrix elements have been extracted from measurements of the total cross section, they can then be used to make predictions for the polarization of  $J/\psi$  produced in leptonproduction without introducing any new free parameters. The measurement of the polarization will be an important check of the NRQCD factorization formalism. The cross section for production of longitudinally polarized  $J/\psi$ , where the polarization axis is the direction of the three-momentum of the  $J/\psi$  in the photon-proton center-of-mass frame, is:

$$\begin{aligned} \sigma(e + p \rightarrow e + \psi_L + X) &= \int \frac{dQ^2}{Q^2} \int dy \int dx f_{g/p}(x) \delta(xys - (2m_c)^2 - Q^2) \\ &\times \frac{2\alpha_s(\mu^2)\alpha^2 e_c^2 \pi^2}{3m_c(Q^2 + (2m_c)^2)} \left\{ \frac{1 + (1-y)^2}{y} \left[ \langle \mathcal{O}_8^\psi(^1S_0) \rangle + 3 \frac{\langle \mathcal{O}_8^\psi(^3P_0) \rangle}{m_c^2} \right] \right. \\ &\quad \left. + \frac{1-y}{y} \frac{48(2m_c)^2 Q^2}{(Q^2 + (2m_c)^2)^2} \frac{\langle \mathcal{O}_8^\psi(^3P_0) \rangle}{m_c^2} \right\}. \end{aligned} \quad (6)$$

The polarization can be measured by studying the angular distribution of the leptons in the leptonic decay of the  $J/\psi$ . If  $\theta$  is defined to be the angle between the momentum of the

leptons in the  $J/\psi$  rest frame and the momentum of the  $J/\psi$  in the photon-proton center of momentum frame, then the decay distribution of the leptons is given by:

$$\frac{d\Gamma(\psi \rightarrow \ell^+ \ell^-)}{d\cos\theta} \propto 1 + \alpha \cos^2\theta \quad (7)$$

where,

$$\alpha = \frac{1 - 3f_L}{1 + f_L}, \quad f_L \equiv \frac{\sigma(\psi_L)}{\sigma(\psi)}. \quad (8)$$

Note that the theoretical prediction depends only on one parameter, the ratio  $R \equiv \langle \mathcal{O}_8^\psi(^3P_0) \rangle / (m_c^2 \langle \mathcal{O}_8^\psi(^1S_0) \rangle)$ . In the limit where  $Q^2, s \gg (2m_c)^2$ , the polarization parameter,  $\alpha$ , goes to zero. This can be seen by inspection of Eqs. (5) and (6).

At  $O(\alpha_s^2)$ ,  $J/\psi$  is produced through the hadronization of a  $c\bar{c}$  pair in either a  $^3S_1$ ,  $^1S_0$ , or  $^3P_J$  configuration. The Feynman diagrams are shown in Fig. 2. Note that only the diagrams in Fig. 2a produce a  $c\bar{c}$  pair in a color-singlet  $^3S_1$  state; all other diagrams produce a color-octet  $c\bar{c}$  pair.

Once again we use the techniques of Ref. [10] to compute the  $J/\psi$  production cross section from the Feynman diagrams shown in Fig 2. The expressions obtained are complicated, so we do not present them here<sup>1</sup>. However, we do report on checks we have made to ensure that that these expressions are correct. First, we have checked that in the  $Q^2 \rightarrow 0$  limit we recover the photoproduction cross section convoluted with the electron splitting function. Second, we numerically compared our color-singlet result to a calculation carried out by Merabet, Mathiot, and Mendez-Galain [11], and find agreement.

#### IV. NON-PERTURBATIVE AND DIFFRACTIVE CONTRIBUTIONS

Before presenting our predictions, we wish to discuss non-perturbative corrections to the NRQCD factorization formalism. Precise determination of the NRQCD matrix elements will

---

<sup>1</sup>The FORTRAN code for generating the differential cross sections presented later in this work is available by request.

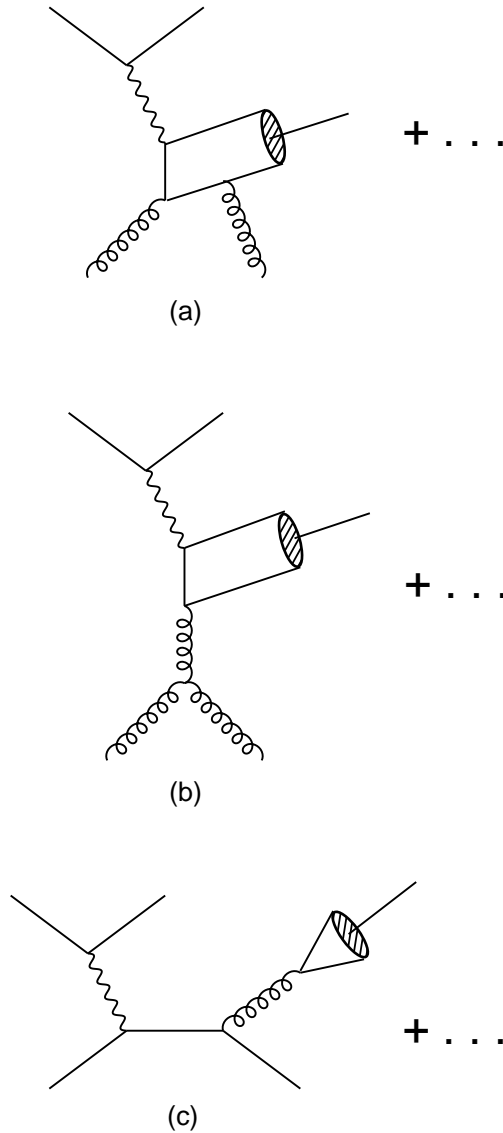


FIG. 2.  $O(\alpha_s^2)$  diagrams for leptoproduction of  $J/\psi$ . There are six diagrams of the type shown in (a), two diagrams of the type shown in (b), and two diagrams of the type shown in (c). The remaining quark diagrams, which are not shown, can be obtained from the diagrams in (b) by replacing the external gluon lines with quarks. Note, that only the diagrams in (a) contribute to the production of a  $c\bar{c}$  pair in a color-singlet  ${}^3S_1$  configuration.

be impossible if these effects are not controlled. In the first part of this section, we consider diffractive lepton production and higher twist corrections to the parton model. In the second part, we discuss the breakdown of the NRQCD velocity expansion near the boundaries of phase space.

### A. Diffraction and higher twist

At the HERA collider at DESY, diffractive processes contribute roughly 40% of the total  $\gamma - p$  cross section [12], and may be an equally important contribution to lepton production of  $J/\psi$ . Moreover, the  $J/\psi$  produced via this mechanism have similar kinematics to  $J/\psi$  produced via the  $O(\alpha_s)$  color-octet contribution.

To understand why diffractive lepton production of  $J/\psi$  is kinematically similar to leading order color-octet production, it is necessary to introduce the following variable:

$$z \equiv \frac{P_p \cdot P_\psi}{P_p \cdot q} . \quad (9)$$

Here  $P_\psi$  is the four-momentum of the  $J/\psi$ . In the proton rest frame  $z = E_\psi/E_\gamma$ . For the process  $e + p \rightarrow e + J/\psi + X$ ,  $z = 1 + t/(s + Q^2)$ , where we neglect the proton mass, and the mass of the final state system  $X$ . Diffractive processes are exponentially suppressed away from  $t = 0$ , where  $z = 1$ .

The short-distance part of the  $O(\alpha_s)$  color-octet contribution leads to the production of a  $c\bar{c}$  pair with no other particles in the final state; hence one would expect  $z = 1$ . However, soft gluons with momentum of order  $m_c v^2$  are radiated during the non-perturbative evolution of the  $c\bar{c}$  into the  $J/\psi$ , resulting in  $z \approx 1 - v^2$ . Thus there is significant overlap of the kinematic regimes of the  $O(\alpha_s)$  color-octet contribution and the diffractive contribution. It is possible to eliminate the diffractive contribution by requiring  $z \ll 1$ ; however the  $O(\alpha_s)$  color-octet mechanism will also be eliminated by such a cut. There are other color-octet contributions at  $z \ll 1$ , but they only occur at higher orders in  $\alpha_s$  where there is no longer a perturbative enhancement of the color-octet term relative to the color-singlet term.

Because diffractive lepton production is characterized by a large scale,  $Q^2$ , this process can be studied using perturbative QCD. In Ref. [13], a perturbative analysis of diffractive lepton production predicts the cross section to fall as  $1/(Q^2 + (2m_c)^2)^3$ , as compared to  $1/(Q^2 + (2m_c)^2)^2$  for the color-octet mechanism. Therefore, at sufficiently large  $Q^2$ , the diffractive contribution should be a negligible correction to our calculation. Furthermore, Ref. [13] predicts that diffractively produced  $J/\psi$  will be longitudinally polarized in the limit  $Q^2 \gg (2m_c)^2$ . As discussed earlier in this paper, the  $O(\alpha_s)$  color-octet mechanism predicts lepton produced  $J/\psi$  to be unpolarized in this limit. Therefore, polarization of the  $J/\psi$  will be a useful tool for distinguishing diffractive production from color-octet mechanisms.

There are also obvious kinematic differences between color-octet and diffractive production which should make it easy to distinguish between the two. The most important distinction is that color-octet production will *not* lead to a rapidity gap in the final state, the hallmark signature of diffractive production. In color-octet production, the octet  $c\bar{c}$  pair produced in the short-distance process must radiate at least one soft gluon before hadronizing into the final state  $J/\psi$ . This soft gluon, with energy in the quarkonium rest frame of order  $m_c v^2$ , will be well-separated in phase space from the proton remnant. A simple computation shows that the invariant mass of the soft gluon emitted by the color-octet  $c\bar{c}$  combined with the proton remnant will be approximately  $vW_{\gamma p}$ , where  $W_{\gamma p}$  is the center-of-mass system energy of the virtual photon and proton. For the H1 experiment at HERA,  $W_{\gamma p}$  ranges between 30 GeV and 150 GeV [14]. If we take  $v^2 = 0.25$ , then for the color-octet contribution to  $e + p \rightarrow e + J/\psi + X$ , we expect  $M_X \geq 15$  GeV. This is obviously much greater than  $M_X = 1$  GeV, what is expected from elastic diffractive events. For diffractive disassociative events,  $M_X$  can be greater than 1 GeV, but the cross section is expected to fall off as  $1/M_X^2$  [14]. By requiring that there be no rapidity gap in the event and that  $M_X \gg 1$  GeV, it should be possible to extract a clean signal for color-octet  $J/\psi$  production.

In addition to the diffractive contribution, we must also consider the possible contribution from higher twist corrections to the parton model. These higher twist effects can be of great importance in quarkonium production calculations.

Well-known factorization theorems [15] show that the inclusive production of a hadron can be written as a convolution of a parton distribution function, a parton scattering cross section calculable in perturbative QCD, and a fragmentation function which describes how the parton produced in the short distance process evolves into the final state hadron. This factorization formula receives higher twist corrections that scale as  $(\Lambda_{QCD}/\mu)^n$ , where  $\mu$  is a characteristic scale of the process. For inclusive single hadron production,  $\mu$  is  $P_\perp$ , the momentum of the hadron transverse to the beam axis. By requiring that  $P_\perp$  be large compared to  $\Lambda_{QCD}$ , we can ensure that predictions of the parton model calculation will be accurate. For quarkonium production, the situation is more complicated because there are two large scales that characterize the process: the mass of the quarkonium state,  $M_H \approx 2m_Q$ , and  $P_\perp$ . If some higher twist corrections are suppressed by  $M_H$  rather than  $P_\perp$ , nonperturbative corrections to the parton model will not diminish as  $P_\perp$  increases. This problem is particularly worrisome in the case of charmonium production, since  $2m_c \approx 3$  GeV, so nonperturbative corrections are not strongly suppressed.

Higher twist corrections to color-singlet *photoproduction* are computed by Ma in Ref. [16]. There it is shown that some of the twist-4 corrections are suppressed only by  $M_\psi^2$ . Since higher twist structure functions are unknown, it is impossible to calculate the size of corrections, but it is clear that, at energies typical of the HERA collider,  $\sqrt{s_{\gamma p}} \approx 100$  GeV, they can be important. Ma states in Ref. [16] that in the case of electroproduction for fixed  $Q^2$  there are no twist-4 corrections that are suppressed by only  $M_\psi^2$ . However, no detailed calculation is given, and until such a calculation is carried out it is not clear what kinematical factor suppresses the higher twist contributions. We assume that higher twist corrections scale like  $\Lambda_{QCD}^2/(Q^2 + (2m_c)^2)$ . An explicit calculation would be most welcome.

## B. Leptoproduction shape functions

Another class of nonperturbative effects is associated with higher orders in the NRQCD velocity expansion [17]. For quarkonium production near the boundaries of phase space,

it is sometimes the case that contributions from NRQCD operators which are higher order in  $v$  are enhanced by kinematical factors. This results in the breakdown of the NRQCD expansion. The crux of the problem is that in the perturbative QCD part of the matching calculation one uses twice the heavy quark mass instead of the quarkonium mass to compute the phase space for the production of the quarkonium meson. The difference between  $2m_Q$  and  $M_H$  is a  $v^2$  correction, which is ignored in leading-order calculations. However, at the boundaries of phase space this difference becomes important, and it is necessary to sum an infinite number of NRQCD matrix elements. This resummation leads to a universal distribution function called a shape function. Because of the universality of the shape functions, it may be possible in the future to test NRQCD by comparing shape functions extracted from different quarkonium production processes. However, in the present paper we are interested in extracting numerical values for the leading color-octet matrix elements. Therefore, we want to make sure that the effects of higher order terms in the NRQCD expansion are genuinely suppressed by powers of  $v^2$  and can be safely neglected.

The leading order contribution for producing  $J/\psi$  through the hadronization of a color-octet  $c\bar{c}$  pair in a  $^1S_0$  configuration is:

$$\begin{aligned} \frac{d\sigma}{dQ^2 dy} &= \int dx f_{g/P}(x) \frac{\sum |\mathcal{M}|^2 d^3 P_\psi}{16\pi x s} \frac{\delta^{(4)}(f + g - f' - P_\psi)}{2E_\psi} \quad (10) \\ &= \int dx S(x, Q^2) \frac{1 + (1-y)^2}{y} \delta\left(y - \frac{Q^2 + (2m_c)^2}{xs}\right) \\ &\quad \times \sum_X \langle 0 | \psi^\dagger T^a \chi | J/\psi + X \rangle \langle J/\psi + X | \chi^\dagger T^a \psi | 0 \rangle, \end{aligned}$$

where

$$S(x, Q^2) = \frac{8\pi f_{g/P}(x) \alpha_s \alpha^2 e_c^2}{9m_c x s Q^2 (Q^2 + (2m_c)^2)}.$$

The  $\mathcal{O}_8^\psi(^3P_0)$  term can be analyzed in an analogous manner. In Eq. (10),  $P_\psi = p_c + p_{\bar{c}}$ , and in evaluating the phase space integral we have used the approximation  $P_\psi = (2m_c, 0, 0, 0)$  in the quarkonium rest frame. If we allow for the  $c$  and  $\bar{c}$  produced in the short distance process to have nonvanishing velocity in the quarkonium rest frame, Eq. (10) becomes:

$$\begin{aligned}
\frac{d\sigma}{dQ^2 dy} &= \int dx f_{g/P}(x) \frac{\sum |\mathcal{M}|^2 d^3 P_\psi}{16\pi x s} \frac{1}{2E_\psi} \delta^{(4)}(f + g - f' - P_\psi - \Lambda(l_c + l_{\bar{c}})) \\
&= \int dx S(x, Q^2) \frac{1 + (1-y)^2}{y} \delta\left(y - \frac{Q^2 + (2m_c)^2}{xs} - \frac{2P_\psi \cdot \Lambda(l_c + l_{\bar{c}})}{xs}\right) \\
&\quad \times \sum_X \langle 0 | \psi^\dagger T^a \chi | J/\psi + X \rangle \langle J/\psi + X | \chi^\dagger T^a \psi | 0 \rangle.
\end{aligned} \tag{11}$$

In this expression,  $l_{c(\bar{c})} = (\sqrt{\vec{l}_{c(\bar{c})}^2 + m_c^2} - m_c, \vec{l}_{c(\bar{c})})$  is the charm (anti-charm) quark four-momentum in the  $J/\psi$  rest frame, and  $\Lambda$  is a boost that takes us from the quarkonium rest frame to the frame in which we are performing the calculation. In order to perform the matching onto NRQCD, the delta function in Eq. (11) is expanded in powers of  $2P_\psi \cdot \Lambda(l_c + l_{\bar{c}})$  and these factors are identified with the matrix elements of the NRQCD operators:

$$\begin{aligned}
\frac{d\sigma}{dQ^2 dy} &= \int dx S(x, Q^2) \frac{1 + (1-y)^2}{y} \sum_n \frac{1}{n!} \delta^{(n)}\left(y - \frac{Q^2 + (2m_c)^2}{xs}\right) \\
&\quad \times \sum_X \langle 0 | \psi^\dagger T^a \chi | J/\psi + X \rangle \langle J/\psi + X | \left(\frac{8m_c^2 i \hat{D}_0}{xs}\right)^n \chi^\dagger T^a \psi | 0 \rangle.
\end{aligned} \tag{12}$$

Here,  $\hat{D}_0 = D_0/(2m_c)$ , where  $D_0$  is the time component of the gauge covariant derivative. The infinite series of operators in Eq. (12) can be summed into the universal shape function:

$$\frac{d\sigma}{dQ^2 dy} = \int dx \int dy_E S(x, Q^2) \frac{1 + (1-y)^2}{y} \delta\left(y - \frac{Q^2 + (2m_c)^2}{xs} - \frac{8m_c^2}{xs} y_E\right) F[{}^1S_0^{(8)}](y_E), \tag{13}$$

where

$$F[{}^1S_0^{(8)}](y_E) = \sum_X \langle 0 | \psi^\dagger T^a \chi | H + X \rangle \langle H + X | \delta(y_E - i\hat{D}_0) \chi^\dagger T^a \psi | 0 \rangle. \tag{14}$$

We now wish to consider the singly differential distribution  $d\sigma/dQ^2$ . Integrating over  $y$  in Eq. (13), and expanding in powers of  $y_E$  we find:

$$\begin{aligned}
\frac{d\sigma}{dQ^2} &= \int dx \int dy \int dy_E S(x, Q^2) \frac{1 + (1-y)^2}{y} F[{}^1S_0^{(8)}](y_E) \delta\left(y - \frac{Q^2 + (2m_c)^2}{xs} - \frac{8m_c^2}{xs} y_E\right) \\
&= \int dx S(x, Q^2) \left( \frac{1 + (1 - y_{LO})^2}{y_{LO}} \langle \mathcal{O}_8({}^1S_0) \rangle - \frac{2 - y_{LO}}{y_{LO}} \Delta F^{(1)} + \frac{2}{y_{LO}} \sum_{n=2}^{\infty} (-)^n \Delta^n F^{(n)} \right).
\end{aligned} \tag{15}$$

In this expression,  $y_{LO} = (Q^2 + (2m_c)^2)/xs$ ,  $\Delta = 2(2m_c)^2/(Q^2 + (2m_c)^2)$ , and



$$F^{(n)} = \int dy_E y_E^n F[{}^1S_0^{(8)}](y_E) \sim v^{2n}.$$

Notice that for  $Q^2 \gg (2m_c)^2$ ,  $\Delta \ll 1$  and the higher order corrections are suppressed by powers of  $\Delta v^2$  instead of  $v^2$ . Thus the corrections associated with non-relativistic treatment of the quarkonium phase space can be made negligible by considering the singly differential distribution  $d\sigma/dQ^2$  at large  $Q^2$ .

Higher order NRQCD corrections associated with the shape function can also be computed for the next-to-leading order color-octet and color-singlet contributions to lepton production of  $J/\psi$ . The calculation is nearly identical to the calculation for photoproduction performed in Ref. [17], so we will merely quote results. The cross section is written in terms of the following variables:  $Q^2$ ,  $y$ ,  $\hat{z}$ ,  $P_\perp$ , and  $\phi$ .  $\hat{z}$  is defined to be  $P_p \cdot P_\psi / P_p \cdot q$ , where the non-relativistic approximation for  $P_\psi$  is used ( $P_\psi = (2m_c, 0, 0, 0)$  in the  $J/\psi$  restframe). This variable is distinct from experimentally observed  $z = P_p \cdot P_\psi / P_p \cdot q$ , where  $P_\psi$  is the observed  $J/\psi$  momentum. We define  $P_\perp$  to be the momentum of the  $J/\psi$  relative to the axis defined by the  $\gamma^*$  three momentum in the  $\gamma^*$ -proton center-of-momentum frame, and  $\phi$  is the azimuthal angle of the  $J/\psi$  about this axis. The differential cross section is given by:

$$\begin{aligned} \frac{d\sigma}{dQ^2 dy d\hat{z}} &= \int d\phi \int dP_\perp^2 \int dy_+ \int dx \frac{f_{g/P}(x) \sum |\mathcal{M}|^2}{2^9 \pi^4 \hat{z} x s} F[{}^{2S+1}L_J^{(1,8)}](y_+) \\ &\times \delta \left( (xys - Q^2)(1 - \hat{z}) - \frac{P_\perp^2 + (2m_c)^2(1 - \hat{z})}{\hat{z}} - \frac{P_\perp^2 + (2m_c)^2(1 - \hat{z})^2}{(2m_c)\hat{z}(1 - \hat{z})} y_+ \right) \end{aligned} \quad (16)$$

Eq. (16) applies equally well to color-octet and color-singlet production, so the quantum numbers of the  $c\bar{c}$  produced in the short-distance process are not specified. It is worth noting that the shape function that appears in Eq. (16) differs from the shape function in Eq. (14):  $\delta(y_E - i\hat{D}_0)$  is replaced with  $\delta(y_+ - in \cdot \hat{D})$ , where  $n^\mu$  is a light-like four vector. Expanding the delta function in Eq. (16) in powers of  $y_+$ , it is easy to see that the moments of the shape function,  $F^{(n)} = \int dy_+ y_+^n F[{}^{2S+1}L_J^{(1,8)}](y_+)$ , are multiplied by a factor  $(1 - \hat{z})^{-n}$ . For  $1 - \hat{z} \leq v^2$ , an infinite number of NRQCD matrix elements are relevant. For this reason, the differential distribution in  $z$  cannot be calculated in the forward region, even if  $Q^2 \gg 4m_c^2$ . However, other differential distributions, such as  $d\sigma/dQ^2$  or  $d\sigma/dP_\perp^2$ , can

be computed because the integration over  $z$  provides sufficient smearing over the singular region.

Based on the analysis presented in this section we have reason to believe that non-perturbative corrections are under control for leptonproduction of  $J/\psi$  at large  $Q^2$ . First, though the size of the diffractive contribution to leptonproduction is difficult to estimate because perturbative QCD calculations of this process are not expected to correctly yield the absolute normalization of the cross section [13], perturbative QCD calculations do predict that diffractive production will be less significant at large  $Q^2$ . In addition, rapidity gaps, the invariant mass squared of the final hadronic state, and the polarization of the  $J/\psi$  produced in diffractive production, all differ in a qualitative way from color-octet production. These observables should allow experimentalists to isolate a clean color-octet signal. Next, higher twist effects are expected to scale as  $\Lambda_{QCD}^2/(Q^2 + (2m_c)^2)$ . Finally, examination of higher order  $v^2$  corrections associated with shape functions gives us insight into which differential distributions can be reliably computed within the NRQCD formalism. The distribution in  $z$  near the kinematic endpoint certainly cannot be predicted in the leading order approximation we consider in this paper. Therefore, we will not attempt to calculate  $d\sigma/dz$ , even though this quantity is often measured in experiments and has been considered by theorists in previous studies. The quantities which we do compute should be insensitive to these corrections.

## V. MATRIX ELEMENT PHENOMENOLOGY

As discussed in the introduction, a naive counting of powers of  $v$  and  $\alpha_s$  tells us that the leading terms in the NRQCD factorization formula for the  $J/\psi$  leptonproduction cross section are the  $O(\alpha_s)$  color-octet contribution, Eq. (3), and the  $O(\alpha_s^2)$  color-singlet contribution. The color-octet contribution depends on the NRQCD production matrix elements  $\langle \mathcal{O}_8^\psi(^1S_0) \rangle$  and  $\langle \mathcal{O}_8^\psi(^3P_0) \rangle$ , and the color-singlet contribution depends on  $\langle \mathcal{O}_1^\psi(^3S_1) \rangle$ . These production matrix elements must be treated as parameters. Thus, before we present our

prediction for  $J/\psi$  leptonproduction we discuss the current status of NRQCD  $J/\psi$  production phenomenology.

The color-singlet matrix element can be determined from the decay  $J/\psi \rightarrow \mu^+\mu^-$  or from lattice calculations [18]. The value determined for  $\langle \mathcal{O}_1^\psi(^3S_1) \rangle$  is shown in Table I.

The values of the color-octet matrix elements  $\langle \mathcal{O}_8^\psi(^1S_0) \rangle$ ,  $\langle \mathcal{O}_8^\psi(^3P_0) \rangle$ , and  $\langle \mathcal{O}_8^\psi(^3S_1) \rangle$  have been extracted from CDF measurements [1] by Cho and Leibovich [5], and by Beneke and Krämer [6]. Neither analysis extracts  $\langle \mathcal{O}_8^\psi(^1S_0) \rangle$  and  $\langle \mathcal{O}_8^\psi(^3P_0) \rangle$  independently, instead they fit a linear combination,  $M_k = \langle \mathcal{O}_8(^1S_0) \rangle + k \langle \mathcal{O}_8(^3P_0) \rangle / m_c^2$ , of the two. In Ref. [5]  $k = 3$ , and in Ref. [6]  $k = 3.5$ . A detailed discussion of theoretical uncertainties in the extraction of these matrix elements is given in Ref. [6], and the results of their fit are shown in Table I. The largest uncertainty is due to scale setting ambiguities. Statistical errors are relatively small, only  $\sim 15\%$  for  $\langle \mathcal{O}_8(^3S_1) \rangle$ , and  $\sim 25\%$  for  $M_{3.5}$ . In this analysis, the charm quark mass is chosen to be 1.5 GeV and errors associated with uncertainty in the choice of this parameter are not considered. Later we will consider errors in our calculation of leptonproduction of  $J/\psi$ , and we will find that uncertainty in the charm quark mass is a much greater source of error than uncertainty due to scale setting ambiguities. While this may not be the case in hadroproduction, we nevertheless feel that uncertainty in charm quark mass is a potentially large source of error which has not been included in the analysis of Ref. [6]. This additional source of error must be kept in mind when considering the extraction of NRQCD matrix elements from this process.

The extraction of  $M_{3.5}$  appears to be particularly unreliable. The contributions to the cross section proportional to the matrix elements  $\langle \mathcal{O}_8^\psi(^1S_0) \rangle$  and  $\langle \mathcal{O}_8^\psi(^3P_0) \rangle$  are subleading except at small transverse momentum,  $P_\perp \leq 5$  GeV. Thus the extraction of these matrix elements is very sensitive to effects which can modify the shape of the  $P_\perp$  spectrum. Specifically, the shape of the proton gluon density at small  $x$  can modify the slope of the  $P_\perp$  distribution at low  $P_\perp$ . This is reflected in the extreme sensitivity of the value of the parameter  $M_{3.5}$  (see Table I) to the choice of the parton distribution function. The authors of [6] take this as evidence that the result of the fit for  $M_{3.5}$  will be unstable to higher order

	$\langle \mathcal{O}_1^\psi(^3S_1) \rangle$ (GeV <sup>3</sup> )	$\langle \mathcal{O}_8^\psi(^3S_1) \rangle$ (10 <sup>-2</sup> GeV <sup>3</sup> )	$M_{3.5}$ (10 <sup>-2</sup> GeV <sup>3</sup> )
$\Gamma(J/\psi \rightarrow \mu^+\mu^-)$	1.1±0.1	–	–
CTEQ4L	–	1.06±0.14 <sup>+1.05</sup> <sub>-0.59</sub>	4.38±1.15 <sup>+1.52</sup> <sub>-0.74</sub>
GRV(1994)LO	–	1.12±0.14 <sup>+0.99</sup> <sub>-0.56</sub>	3.90±1.14 <sup>+1.46</sup> <sub>-1.07</sub>
MRS(R2)	–	1.40±0.22 <sup>+1.35</sup> <sub>-0.79</sub>	10.9±2.07 <sup>+2.79</sup> <sub>-1.26</sub>

TABLE I.  $M_{3.5}$  is the linear combination  $\langle \mathcal{O}_8(^1S_0) \rangle + 3.5\langle \mathcal{O}_8(^3P_0) \rangle/m_c^2$ . The color-singlet matrix element is determined from the decay rate for  $J/\psi \rightarrow \mu^+\mu^-$ . The color-octet matrix elements are determined from a fit to CDF data performed in Ref. [6]. First error is statistical, second is due to scale uncertainty.

corrections and nonperturbative effects that will modify the  $P_\perp$  distribution at low  $P_\perp$ . As a result they conclude that  $\langle \mathcal{O}_8^\psi(^1S_0) \rangle$  and  $\langle \mathcal{O}_8^\psi(^3P_0) \rangle$  are not reliably extracted from CDF data.

As discussed in the introduction  $\langle \mathcal{O}_8^\psi(^1S_0) \rangle$  and  $\langle \mathcal{O}_8^\psi(^3P_0) \rangle$  can be extracted from experimental data on photoproduction and low energy hadroproduction of  $J/\psi$ . However, theoretical uncertainties only allow for an order of magnitude estimate of the color-octet matrix elements.

## VI. RESULTS

Our study of leptonproduction of  $J/\psi$  at large  $Q^2$  will show that this process can provide a more accurate extraction of  $\langle \mathcal{O}_8^\psi(^1S_0) \rangle$  and  $\langle \mathcal{O}_8^\psi(^3P_0) \rangle$  than hadroproduction or photoproduction. Unfortunately, at this time, there does not exist appropriate data to which a reliable fit can be made. There does exist data on  $J/\psi$  muoproduction [19]; a fit to the EMC data was carried out in Ref. [20]. However, we must caution that this data was taken with low to moderate values of  $Q^2$ . In this regime, we expect large non-perturbative corrections to the NRQCD factorization formalism. More importantly, as we will see below, in the low  $Q^2$  region the perturbative calculation suffers errors, due to the uncertainty in the charm

quark mass parameter. Therefore, we will not make a fit to the existing leptonproduction data. Instead, we will choose two sets of reasonable values for  $\langle \mathcal{O}_8^\psi(^1S_0) \rangle$ , and  $\langle \mathcal{O}_8^\psi(^3P_0) \rangle$  in order to make predictions.

In the results presented below, we choose either  $\langle \mathcal{O}_8^\psi(^1S_0) \rangle = 0.01 \text{ GeV}^3$  and  $\langle \mathcal{O}_8^\psi(^3P_0) \rangle / m_c^2 = 0.005 \text{ GeV}^3$ , inspired by the order-of-magnitude estimates presented in Table I, and in accordance with NRQCD  $v$ -scaling rules, or  $\langle \mathcal{O}_8^\psi(^1S_0) \rangle = 0.04 \text{ GeV}^3$ , and  $\langle \mathcal{O}_8^\psi(^3P_0) \rangle / m_c^2 = -0.003 \text{ GeV}^3$ , which is consistent with the fit to low  $Q^2$  EMC data carried out in Ref. [20]. In addition, we require  $Q^2 > 4 \text{ GeV}^2$ . This should reduce errors from higher order perturbative QCD terms and from higher twist effects. We also assume that experiments at HERA are most likely to make precision measurements of  $J/\psi$  leptonproduction, so we choose the center-of-mass energy to be  $\sqrt{s} = 300 \text{ GeV}$ , and require  $30 \text{ GeV} < W_{\gamma p} < 150 \text{ GeV}$ , where  $W_{\gamma p}^2 = (P_p + q)^2$ .

Given the above conditions, we calculate the  $O(\alpha_s)$  color-octet contribution to the  $J/\psi$  leptonproduction cross section, and the  $O(\alpha_s^2)$  color-singlet contribution to the cross section. The results are presented in Table II for two sets of kinematic cuts:  $Q^2 > 4 \text{ GeV}^2$ , and  $Q^2 > 4 \text{ GeV}^2$ ,  $P_\perp^2 > 4 \text{ GeV}^2$ , where  $P_\perp$  is the transverse momentum of the  $J/\psi$  in the HERA lab frame. The color-octet result is for the first (second) choice of  $\langle \mathcal{O}_8^\psi(^1S_0) \rangle$  and  $\langle \mathcal{O}_8^\psi(^3P_0) \rangle$  given above. Note that with no  $P_\perp$  cut the color-singlet contribution is  $\sim 1/4$  the size of the color-octet contribution, while with a  $P_\perp$  cut it is  $\sim 1/5$  the size of the color-octet contribution. For either choice of color-octet matrix element values the  $O(\alpha_s^2)$  color-singlet contribution is small compared to the  $O(\alpha_s)$  color-octet contribution.

If we consider final states in which a gluon jet is well separated from the  $J/\psi$ , there is no contribution to the cross section from the  $O(\alpha_s)$  color-octet term. This is because the  $O(\alpha_s)$  color-octet contribution produces  $J/\psi$  through the emission of soft gluons from the  $c\bar{c}$  pair produced in the hard scattering. These gluons have less than 1 GeV of momentum in the  $J/\psi$  rest frame. However, there will still be a color-octet contribution from  $O(\alpha_s^2)$  tree level diagrams. To isolate events in which the gluon jet is well separated from the  $J/\psi$ , we require that  $(P_\perp^{\gamma P})^2 > 2 \text{ GeV}^2$  and  $z < 0.8$ .  $P_\perp^{\gamma P}$  is the momentum of the  $J/\psi$  transverse

Cuts	$O(\alpha_s)$ color-octet	$O(\alpha_s^2)$ color-singlet	$O(\alpha_s^2)$ color-octet
$Q^2 > 4 \text{ GeV}^2$	331 (226) pb	89 pb	–
$Q^2, P_\perp^2 > 4 \text{ GeV}^2$	290 (200) pb	40 pb	–
$(P_\perp^{\gamma P})^2 > 2 \text{ GeV}^2, z < 0.8$	–	13 pb	8 pb

TABLE II. The  $O(\alpha_s)$  color-octet contribution to the  $J/\psi$  leptonproduction cross section for  $\langle \mathcal{O}_8^\psi(1S_0) \rangle = 0.01 \text{ GeV}^2$  and  $\langle \mathcal{O}_8^\psi(3P_0) \rangle / m_c^2 = 0.005 \text{ GeV}^2$  ( $\langle \mathcal{O}_8^\psi(1S_0) \rangle = 0.04 \text{ GeV}^2$  and,  $\langle \mathcal{O}_8^\psi(3P_0) \rangle / m_c^2 = 0.005 \text{ GeV}^2$ ), the  $O(\alpha_s^2)$  color-singlet contribution, and the  $O(\alpha_s^2)$  color-octet contribution. The results are given for three different sets of kinematic cuts. Only the  $O(\alpha_s)$  color-octet calculation and the  $O(\alpha_s^2)$  color-singlet calculation are valid in the region of the first two sets of cuts. There are only  $O(\alpha_s^2)$  contributions in region of the third set of cuts. Note theoretical errors are not included.

to the axis defined by photon three-momentum in the photon-proton center-of-momentum frame. The result of this calculation is shown in Table II. The  $O(\alpha_s^2)$  color-octet diagrams contribute about 40% of the total cross section. We do not show differential distributions in  $P_\perp^2$ , rapidity, and  $Q^2$ , but report that the shape of these distributions is roughly the same for both  $O(\alpha_s^2)$  color-octet and  $O(\alpha_s^2)$  color-singlet contributions. Therefore, inclusion of color-octet mechanisms only serves to change the overall normalization of the total cross section in this region of phase space. Since the overall normalization is already uncertain in a leading order calculation, we do not regard events with  $J/\psi$  and a gluon jet as particularly interesting for measuring color-octet matrix elements.

In Fig. 3, we show the  $O(\alpha_s)$  color-octet contribution (upper histograms) and the  $O(\alpha_s^2)$  color-singlet contribution (lower histograms) to the differential cross section as a function of  $Q^2$ . The solid histograms are without a  $P_\perp^2$  cut, and the dashed histograms are with a  $P_\perp^2$  cut of  $4 \text{ GeV}^2$ . In generating the curves we used  $\mu^2 = Q^2 + (2m_c)^2$ ,  $m_c = 1.5 \text{ GeV}$ , and  $\langle \mathcal{O}_8^\psi(1S_0) \rangle = 0.01 \text{ GeV}^3$ ,  $\langle \mathcal{O}_8^\psi(3P_0) \rangle / m_c^2 = 0.005 \text{ GeV}^3$ . Next, we study the error in our calculation that results from uncertainty in the choice of renormalization and factorization scales. In Fig. 4, we show the  $O(\alpha_s)$  color-octet differential cross section as a function of

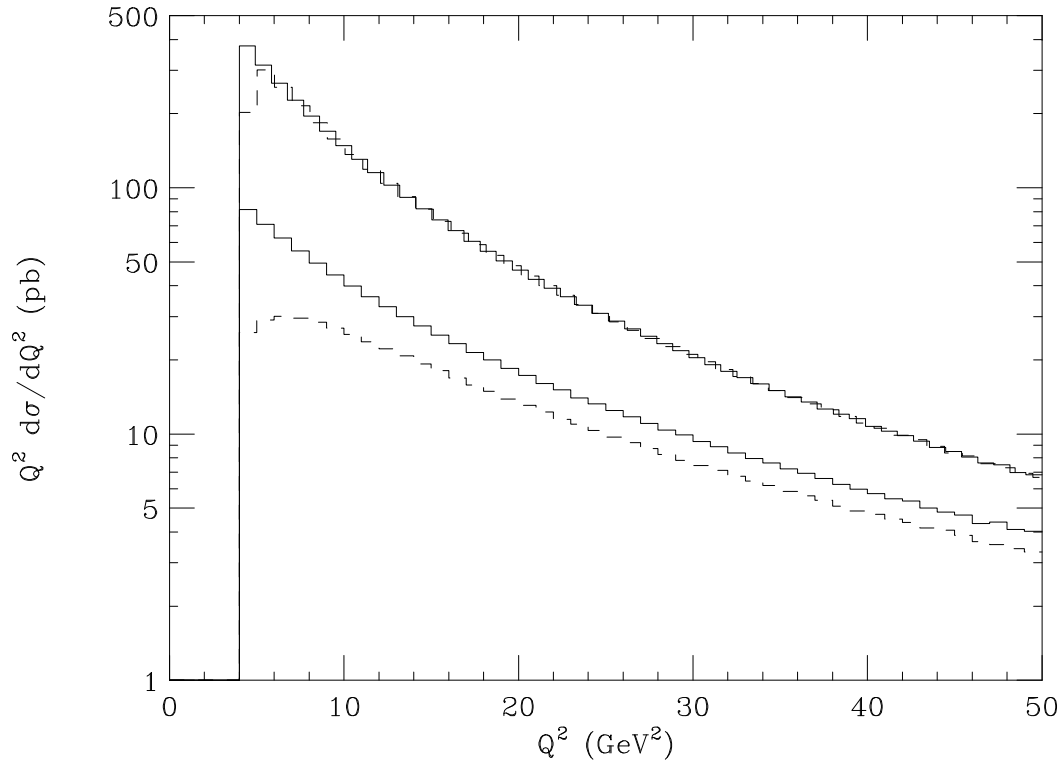


FIG. 3.  $O(\alpha_s)$  color-octet (upper histograms) and  $O(\alpha_s^2)$  color-singlet (lower histograms) contributions to the differential cross section as a function of  $Q^2$  for two sets of kinematic cuts. The solid histograms were generated with a  $Q^2$  cut of  $4 \text{ GeV}^2$ , and the dashed histograms were generated cutting on both  $Q^2 > 4 \text{ GeV}^2$ , and  $P_{\perp}^2 > 4 \text{ GeV}^2$ .

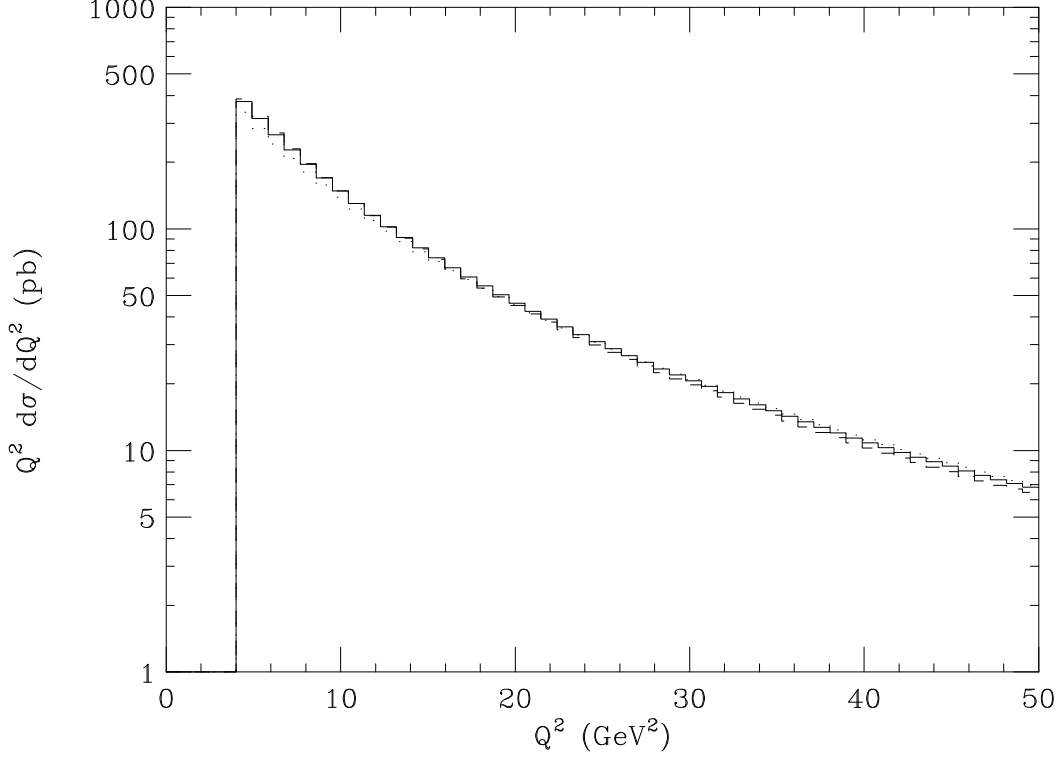


FIG. 4.  $O(\alpha_s)$  color-octet differential cross section as a function of  $Q^2$  for three different choices of scale:  $\mu^2 = Q^2 + (2m_c)^2$  (solid histogram),  $\mu^2/4$  (dotted histogram), and  $4\mu$  (dashed histogram).

$Q^2$  for three choices of the renormalization and factorization scale:  $\mu^2 = Q^2 + (2m_c)^2$  (solid histogram),  $\mu^2/4$  (dotted histogram), and  $4\mu^2$  (dashed histogram). If we were to fit this result to experimental data the scale uncertainty would result in a theoretical uncertainty of about  $^{+3\%}_{-11\%}$  at  $Q^2 = 4 \text{ GeV}^2$ , and  $^{+2\%}_{-5\%}$  at  $Q^2 = 50 \text{ GeV}^2$  in determining the values of the color-octet matrix elements. These small errors give us confidence that higher order perturbative corrections to the leading color-octet production mechanisms are under control.

In Fig. 5, we study the error in our prediction for the  $O(\alpha_s)$  color-octet differential cross section resulting from uncertainty in the determination of the charm quark mass. The three histograms in the figure correspond to three different choices of  $m_c$ :  $m_c = 1.3 \text{ GeV}$  (dotted histogram),  $m_c = 1.5 \text{ GeV}$  (solid histogram), and  $m_c = 1.7 \text{ GeV}$  (dashed histogram). The error in our prediction for the cross section, as defined by

$$\epsilon = \left( \frac{d\sigma(m_c)}{dQ^2} - \frac{d\sigma(m_c = 1.5 \text{ GeV})}{dQ^2} \right) / \frac{d\sigma(m_c = 1.5 \text{ GeV})}{dQ^2},$$

is plotted in Fig. 6 for  $m_c = 1.3 \text{ GeV}$  (dashed line) and  $1.7 \text{ GeV}$  (dotted line). Though there



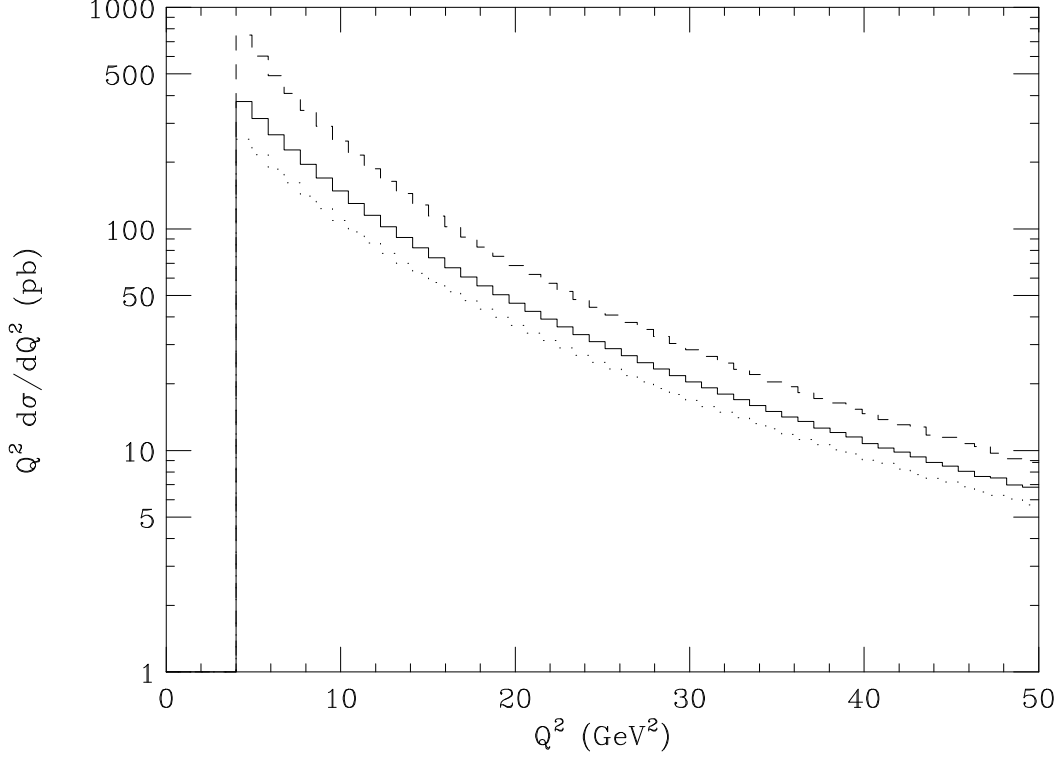


FIG. 5.  $O(\alpha_s)$  color-octet differential cross section as a function of  $Q^2$  for three different choices of  $m_c$ .  $m_c = 1.3$  GeV (dotted histogram),  $m_c = 1.5$  GeV (solid histogram), and  $m_c = 1.7$  GeV (dashed histogram).

is some improvement as  $Q^2$  is increased, the error is still  $^{+60\%}_{-25\%}$  at  $Q^2 = 10$  GeV<sup>2</sup>. This is much greater than errors we expect to receive from higher orders in perturbation theory and higher twist effects, so the uncertainty in the charm quark mass dominates the theoretical error in our prediction.

In addition to the  $Q^2$  distribution, we have also calculated the  $P_{\perp}^2$  distribution shown in Fig. 7, and the rapidity distribution shown Fig. 8. The rapidity of the  $J/\psi$ , is defined to be:

$$y = \frac{1}{2} \ln \left( \frac{E + P_z}{E - P_z} \right),$$

where  $E$  and  $P_z$  are the energy and  $z$ -component of the  $J/\psi$  three-momentum measured in the photon-proton center-of-momentum frame with the  $z$ -axis defined by the photon three-momentum in that frame. We only present results for one choice of scale,  $\mu^2 = Q^2 + (2m_c)^2$ , one choice of charm quark mass,  $m_c = 1.5$  GeV, and for  $\langle \mathcal{O}_8^{\psi}(^1S_0) \rangle = 0.01$  GeV<sup>3</sup>,  $\langle \mathcal{O}_8^{\psi}(^3P_0) \rangle / m_c^2 = 0.005$  GeV<sup>3</sup>. Note that in Fig. 8 there is no  $P_{\perp}$  cut. The sharp fall off of

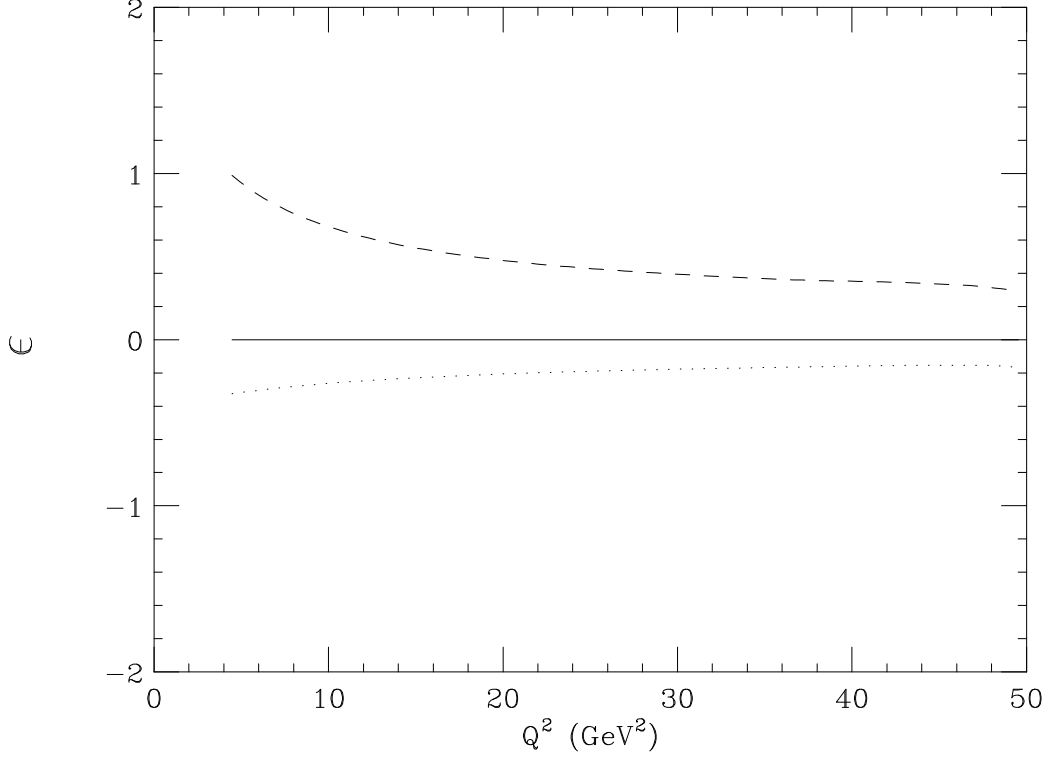


FIG. 6. Theoretical error due to uncertainty in charm quark mass as a function of  $Q^2$ . Error is plotted for  $m_c = 1.3$  GeV and  $m_c = 1.7$  GeV.

the distribution at  $P_{\perp}^2 \sim 3$  GeV<sup>2</sup> is due to the  $Q^2 > 4$  GeV<sup>2</sup> cut. The  $P_{\perp}^2$  and  $y$  distributions suffer considerable error due to the charm quark mass uncertainty. In the case of the  $P_{\perp}^2$  distribution, the errors are similar in size to the  $Q^2$  distribution, and, like the  $Q^2$  distribution, decrease slightly as  $P_{\perp}^2$  is increased. For the  $y$  distribution, the error is roughly  $^{+50\%}_{-25\%}$ , and is independent of  $y$ .

Once the color-octet matrix elements have been determined from leptonproduction of unpolarized  $J/\psi$ , it is possible to make definite predictions for the production of polarized  $J/\psi$ . The expression for the polarization parameter,  $\alpha$ , is given in Eq. (8) and depends only on the ratio of color-octet matrix elements  $R \equiv \langle \mathcal{O}_8^{\psi}(^3P_0) \rangle / (m_c^2 \langle \mathcal{O}_8^{\psi}(^1S_0) \rangle)$ . In Fig. 9, we plot  $\alpha$  as a function of  $Q^2$ , choosing  $\mu^2 = Q^2 + (2m_c)^2$ , and  $m_c = 1.5$  GeV. Plots are shown for  $R = 1.0, 0.5, 0.25, -0.075$ . If the  $c\bar{c}$  produced in the short distance process is in a  $^1S_0$  state, the  $J/\psi$  will be unpolarized, so we expect  $\alpha = 0$  when  $R = 0$ . Positive values of  $R$  lead to slightly longitudinally polarized  $J/\psi$  ( $\alpha < 0$ ), while if  $R < 0$  (i.e.  $\langle \mathcal{O}_8^{\psi}(^3P_0) \rangle < 0$ ) the

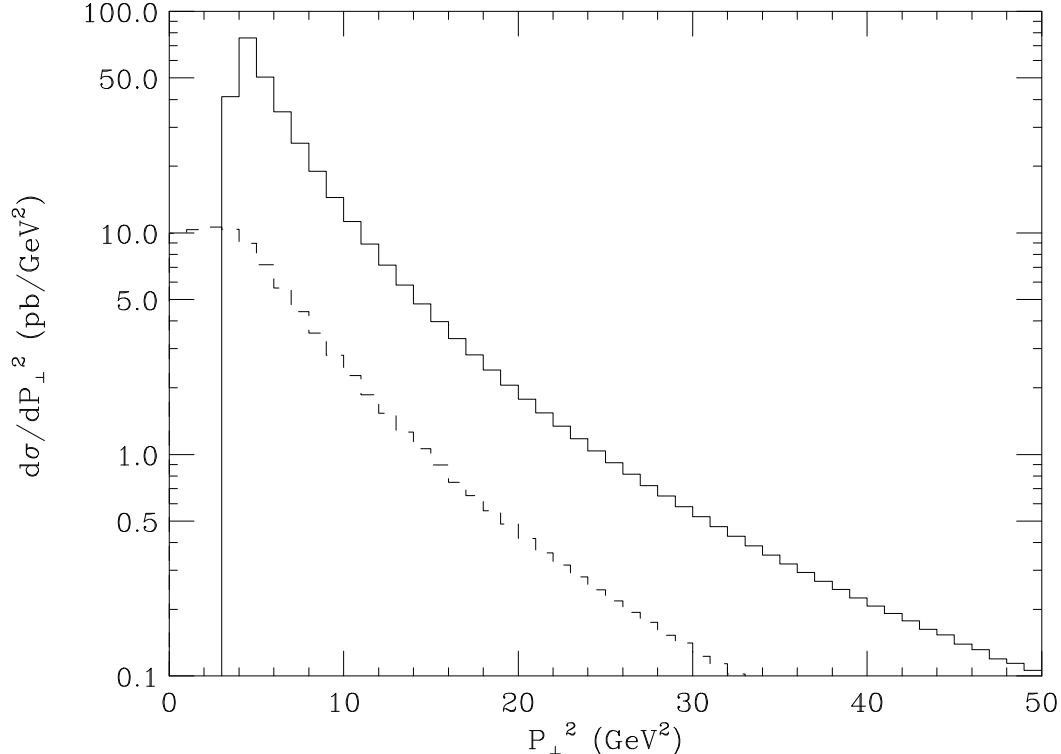


FIG. 7. Differential cross section as a function of  $P_{\perp}$ . Solid -  $O(\alpha_s)$  color-octet; dashed -  $O(\alpha_s^2)$  color-singlet. We require  $Q^2 > 4 \text{ GeV}^2$ ; no  $P_{\perp}$  cut is imposed.

$J/\psi$  emerges with slightly transverse polarization. The error due to the uncertainty in the charm quark mass is significant, but not as large as the errors in the  $P_{\perp}$  or  $y$  distributions. To illustrate this, we plot the polarization in the case of  $R = 0.5$  for three different values of  $m_c$  in Fig. 10. The error is largest at large values of  $Q^2$  where it is approximately  $^{+20\%}_{-5\%}$ . Note that we have only included the  $O(\alpha_s)$  color-octet contribution. Since the  $O(\alpha_s^2)$  color-singlet mechanism contributes about 25% of the total cross section, its effect on the polarization needs to be included before detailed comparison with experiment can be made.

In summary, the total cross section for leptonproduction of  $J/\psi$  is dominated by leading order color-octet terms; the  $O(\alpha_s^2)$  color-singlet term contributes only 20-25% of the total cross section. An accurate measurement of the distribution  $d\sigma/dQ^2$  will, thus, allow for an independent determination of  $\langle \mathcal{O}_8^{\psi}(^1S_0) \rangle$  and  $\langle \mathcal{O}_8^{\psi}(^3P_0) \rangle$ . As discussed in section IV, nonperturbative errors are expected to be small at large  $Q^2$ . For  $Q^2 > 4 \text{ GeV}^2$  higher twist effects result in an error of less than 8%. In addition we estimate the error due to the scale

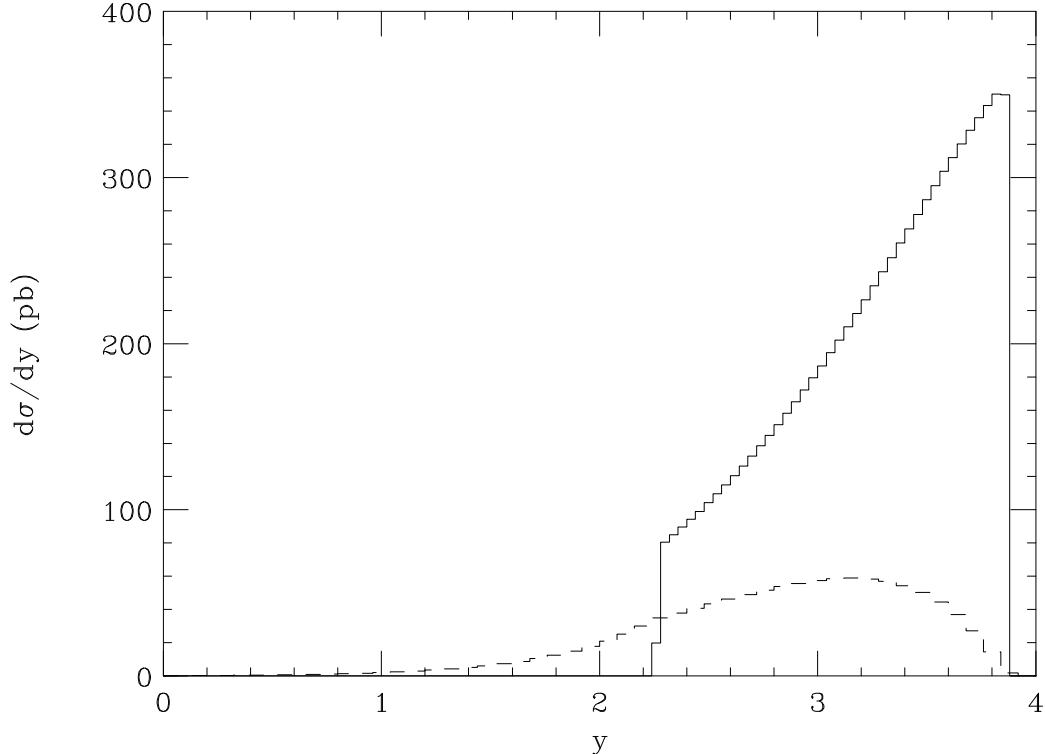


FIG. 8. Differential cross section as a function of rapidity ( $y$ ). Solid -  $O(\alpha_s)$  color-octet; dashed -  $O(\alpha_s^2)$  color-singlet. We impose the cut  $Q^2 > 4 \text{ GeV}^2$

uncertainty; we find it is less than 10%. Finally we estimate the error due to the uncertainty in the determination of the charm quark mass, and find it to be the dominant error. One must require  $Q^2 > 10 \text{ GeV}^2$  for the error to be less than 50%. Errors in the extraction of  $\langle \mathcal{O}_8^\psi(1S_0) \rangle$  and  $\langle \mathcal{O}_8^\psi(3P_0) \rangle$  from photoproduction ( $Q^2 = 0$ ) are obviously greater than 100%. The errors that arise in extractions from hadroproduction reported in Ref. [6] are greater than 100%, and do not even include error due to uncertainty in the charm quark mass. Therefore, measurement of leptonproduction of  $J/\psi$  at  $Q^2 \geq 10 \text{ GeV}^2$  will be a great improvement over existing extractions. Nevertheless, it is somewhat disappointing that our prediction is dominated by the error due to the uncertainty in the charm quark mass since it cannot be systematically reduced by doing higher order perturbative QCD calculations.

Once  $\langle \mathcal{O}_8^\psi(1S_0) \rangle$  and  $\langle \mathcal{O}_8^\psi(3P_0) \rangle$  are determined, distributions in  $P_\perp^2$  and rapidity, as well as the polarization of the  $J/\psi$ , can also be predicted. The polarization of  $J/\psi$  is least sensitive to errors associated with the uncertainty in the charm quark mass. Thus, an

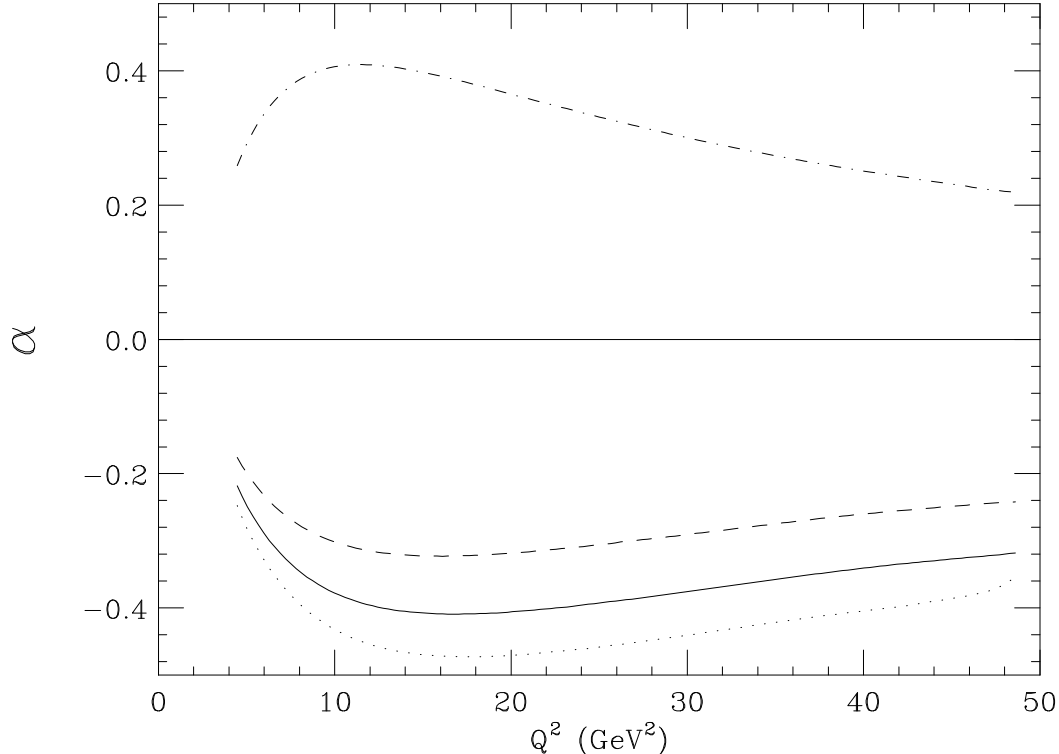


FIG. 9. Polarization parameter  $\alpha$  as function of  $Q^2$ . Dashed line -  $R = 0.25$ ; Solid line -  $R = 0.5$ ; Dotted line -  $R = 1.0$ ; Dashed-dotted line -  $R = -0.075$

experimental measurement of the polarization will be an important test of the NRQCD factorization formalism.

In addition, we have shown that the production of  $J/\psi$  with a well separated gluon jet occurs only at  $O(\alpha_s^2)$ , and makes a small contribution to the total cross section. For these final states, the color-octet contribution is suppressed, and only modifies the normalization, but not the shapes of distributions. For this reason, we do not feel that production of  $J/\psi$  in association with a hard jet will shed any light on color-octet mechanisms.

## VII. CONCLUSION

In this paper, we studied leptonproduction of  $J/\psi$  at large  $Q^2$ , and found that the cross section is dominated by  $O(\alpha_s)$  color-octet production mechanisms. Thus, by measuring the total cross section as a function of  $Q^2$ , it is possible to obtain measurements of the color-octet matrix elements  $\langle \mathcal{O}_8^\psi(^1S_0) \rangle$  and  $\langle \mathcal{O}_8^\psi(^3P_0) \rangle$ . Neither of these has been determined to

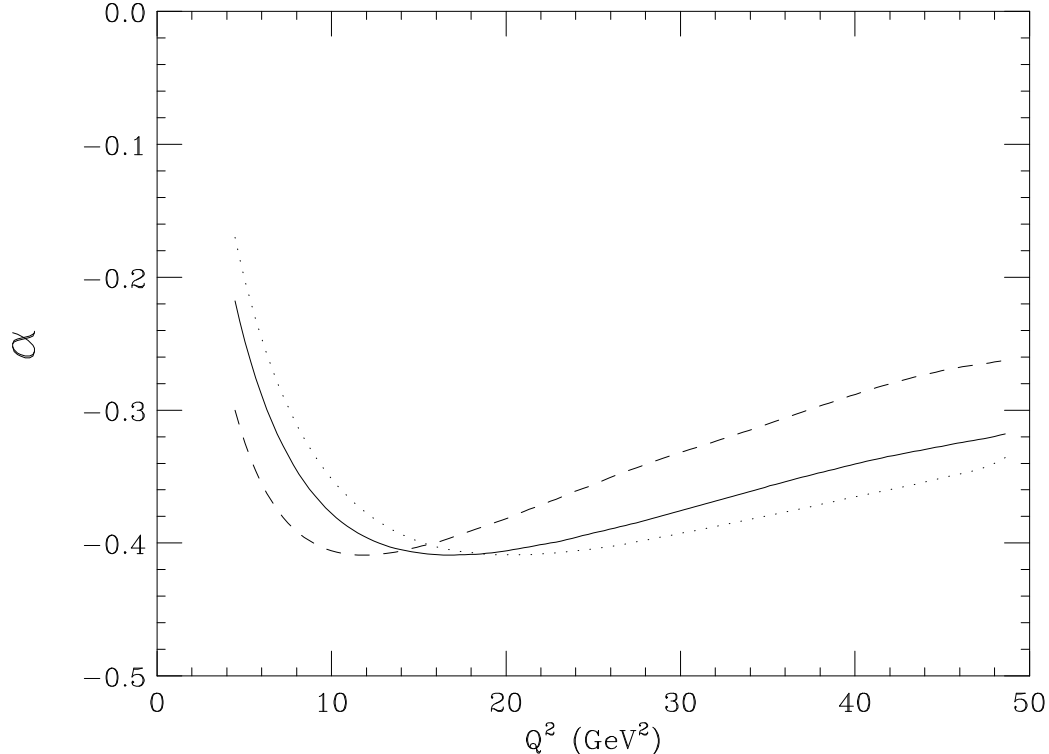


FIG. 10. Polarization parameter  $\alpha$  as function of  $Q^2$ .  $R = 0.5$ ; Solid line -  $m_c = 1.5\text{GeV}$ ; Dotted line -  $m_c = 1.7\text{GeV}$ ; Dashed line -  $m_c = 1.3\text{GeV}$ .

better than an order of magnitude. The dominant error is due to the uncertainty in the value of the charm quark mass. This results in roughly a 50% uncertainty in the prediction for the differential cross section for  $Q^2 > 10 \text{ GeV}^2$ . We, therefore, estimate that  $\langle \mathcal{O}_8^\psi(^1S_0) \rangle$  and  $\langle \mathcal{O}_8^\psi(^3P_0) \rangle$  can be measured in  $J/\psi$  leptonproduction at about the 50% level.

In addition, we pointed out that once the color-octet matrix elements have been measured it is possible to make a parameter free prediction of the polarization of leptonproduced  $J/\psi$ . This will provide an important test of the NRQCD factorization formalism.

As a result of the work presented in this paper we conclude that leptonproduction of unpolarized  $J/\psi$  at  $Q^2 > 10 \text{ GeV}^2$  will provide a much better determination of the color-octet matrix elements  $\langle \mathcal{O}_8^\psi(^1S_0) \rangle$  and  $\langle \mathcal{O}_8^\psi(^3P_0) \rangle$  than currently available. In addition a measurement of the polarization of leptonproduced  $J/\psi$  will provide an important test of the NRQCD factorization formalism. We would, therefore, encourage an experimental measurement of  $J/\psi$  leptonproduction at large  $Q^2$ .

We would like to thank Adam Falk for countless consultations, suggestions, and for reading over the final drafts of the paper. In addition we would like to thank David Rainwater for help with the Monte Carlo integration routines. The work of S.F. was supported in part by the U.S. Department of Energy under Grant no. DE-FG02-95ER40896, in part by the University of Wisconsin Research Committee with funds granted by the Wisconsin Alumni Research Foundation. The work of T.M. was supported by the National Science Foundation under Grant No. PHY-9404057.

## REFERENCES

- [1] For a review of experimental aspects of quarkonia production, see Sansoni, A. (CDF Collaboration), Nucl. Phys. **A610**, 373c (1996).
- [2] For an extensive review of the color-singlet model, see G. A. Schuler, CERN-TH-7170-94, hep-ph/9403387 (unpublished).
- [3] G.T. Bodwin, E. Braaten, and G.P. Lepage, Phys. Rev. D **51** 1125 (1995).
- [4] G.P. Lepage, L. Magnea, C. Nakhleh, U. Magnea, and K. Hornbostle, Phys. Rev. D **46**, 4052 (1992).
- [5] P. Cho and A. Leibovich, Phys. Rev. D **53**, 150 (1996); **53**, 6203 (1996).
- [6] M. Beneke and M. Krämer, Phys. Rev. D **55**, 5269 (1997); M. Beneke, Report No. CERN-TH/97-55, hep-ph/9703429 (unpublished)
- [7] J. Amundson, S. Fleming, and I. Maksymyk, Report No. UTTG-10-95, hep-ph/9601298 (unpublished); M. Cacciari and M. Krämer, Phys. Rev. Lett. **76**, 4128 (1996); P. Ko, J. Lee, and H.S. Song, Phys. Rev. D **54**, 4312 (1996).
- [8] M. Beneke and I. Rothstein, Phys. Rev. D **54**, 2005 (1996); S. Gupta and R. Sridhar, *ibid.* **54**, 5455 (1996); *ibid.* **55**, 2650 (1997); W.K. Tang and M. Vanttinen, *ibid.* **54**, 4349 (1996); *ibid.* **53**, 4851 (1996).
- [9] H.W. Huang and K.T. Chao, Phys. Rev. D **55** 244, (1997); E. Braaten and Y.Q. Chen, Phys. Rev. D **55**, 7152 (1997).
- [10] E. Braaten and Y. Chen, Phys. Rev. **D54**, 3216 (1996); S. Fleming and I. Maksymyk, *ibid.* **54**, 3608 (1996).
- [11] H. Merabet, J.-F. Mathiot, R. Mendez-Galain, Z. Phys C **62**, 639 (1994).
- [12] Cartiglia, Nicolo, Report No. hep-ph/97032245 (unpublished).



- [13] S. J. Brodsky, L. Frankfurt, J. F. Gunion, A.H. Mueller, and M. Strikman, Phys. Rev. D **50**, 3134 (1994); M.G. Ryskin, R.G. Roberts, A.D. Martin, and E.M. Levin, Report No. RAL-TR-95-065, hep-ph/9511228 (unpublished).
- [14] H1 Collaboration, S. Aid, *et. al.*, Nucl. Phys.**B468**, 3 (1996).
- [15] J. C. Collins, D. E. Soper, Ann. Rev. Part. Sci. 37, (1987) 383.
- [16] J. P. Ma, Report No. RCHEP-96/07, hep-ph/9705445, (unpublished).
- [17] M. Beneke, I. Z. Rothstein, and M. B. Wise, Report No. CERN-TH/97-86, hep-ph/9705286, (unpublished).
- [18] G.T. Bodwin, D.K. Sinclair, and S. Kim, Phys. Rev. Lett. **77**, 2376 (1996).
- [19] EMC Collaboration, J.J. Aubert, *et. al.*, Nucl. Phys. **B213**, 1 (1983); D. Allasia *et al.* Phys. Lett. **258B**, 493 (1991); Ch. Moriotti, Nucl. Phys. **A532**, 437 (1991).
- [20] S. Fleming, Report No. hep-ph/9610372 (unpublished).